Prevention of apoptosis averts glomerular tubular disconnection and podocyte loss in proteinuric kidney disease

OPEN

Ievgeniia Burlaka[1,4], Linnéa M. Nilsson[2,4], Lena Scott[1,4], Ulla Holtbäck[1], Ann-Christine Eklöf[1], Agnes B. Fogo[3], Hjalmar Brismar[1,2] and Anita Aperia[1]

[1]*Science for Life Laboratory, Department of Women's and Children's Health, Karolinska Institutet, Solna, Sweden;* [2]*Science for Life Laboratory, Department of Applied Physics, Royal Institute of Technology, Solna, Sweden; and* [3]*Department of Pathology, Microbiology and Immunology, Vanderbilt University Medical Center, Nashville, Tennessee, USA*

There is a great need for treatment that arrests progression of chronic kidney disease. Increased albumin in urine leads to apoptosis and fibrosis of podocytes and tubular cells and is a major cause of functional deterioration. There have been many attempts to target fibrosis, but because of the lack of appropriate agents, few have targeted apoptosis. Our group has described an ouabain-activated Na,K-ATPase/IP3R signalosome, which protects from apoptosis. Here we show that albumin uptake in primary rat renal epithelial cells is accompanied by a time- and dose-dependent mitochondrial accumulation of the apoptotic factor Bax, down-regulation of the antiapoptotic factor Bcl-xL and mitochondrial membrane depolarization. Ouabain opposes these effects and protects from apoptosis in albumin-exposed proximal tubule cells and podocytes. The efficacy of ouabain as an antiapoptotic and kidney-protective therapeutic tool was then tested in rats with passive Heymann nephritis, a model of proteinuric chronic kidney disease. Chronic ouabain treatment preserved renal function, protected from renal cortical apoptosis, up-regulated Bax, down-regulated Bcl-xL, and rescued from glomerular tubular disconnection and podocyte loss. Thus we have identified a novel clinically feasible therapeutic tool, which has the potential to protect from apoptosis and rescue from loss of functional tissue in chronic proteinuric kidney disease.

Kidney International (2016) ■, ■–■; http://dx.doi.org/10.1016/j.kint.2016.03.026

KEYWORDS: albuminuria; apoptosis; cell signaling; chronic kidney disease; ouabain; podocyte; proximal tubule; sodium potassium adenosine triphosphatase; a-tubular glomeruli

Correspondence: *Anita Aperia, Department of Women's and Children's Health Science for Life Laboratory, Box 1031, S-171 21 Solna, Sweden. E-mail: Anita.Aperia@ki.se; or Lena Scott, Department of Women's and Children's Health Science for Life Laboratory, Box 1031, S-171 21 Solna, Sweden. E-mail: Lena.Scott@ki.se*

[4]These authors contributed equally to this work.

Received 21 September 2015; revised 19 February 2016; accepted 10 March 2016

Chronic kidney disease (CKD) is a rapidly increasing world-wide public health problem.[1] CKD results from many causes, including diabetes, glomerulonephritis, hypoxia, hypertension, infections, and polycystic kidney disease. Most forms of CKD are progressive[1–3] and characterized by disrupted glomerular perm-selectivity, albuminuria, loss of podocytes, interstitial fibrosis, and glomerular-tubular disconnection.[4–9] Albuminuria, a well-documented predictor of progressive loss of kidney function, is considered a cause of kidney damage and loss of function.[10–13] The nature of albumin toxicity has been extensively studied in the past decade, and it is well recognized that prolonged exposure of renal tubular cells to albumin results in apoptosis and fibrosis,[14–18] but their interrelationship is not yet fully understood. There are several ongoing trials aimed at halting progression of CKD using drugs targeted to inhibit profibrotic and/or stimulate antifibrotic molecular pathways,[19–22] but there are few attempts to target the apoptotic process, mainly because of lack of nontoxic agents.

Apoptosis is triggered either via an extrinsic pathway stimulated by activation of plasma membrane death receptors or via an intrinsic mitochondrial pathway. The intrinsic apoptotic pathway is controlled by the family of B-cell lymphoma (Bcl)-2 proteins. The mitochondrial apoptotic pathway is initiated by activation of Bax, a prominent pro-apoptotic member of the Bcl-2 family, to the outer mitochondrial membrane, where it oligomerizes and penetrates the inner mitochondrial membrane. This results in release of cytochrome C and caspase activation, the apoptotic executors. B-cell lymphoma–extra large (Bcl-xL), a prominent anti-apoptotic member of the Bcl-2 family, counteracts Bax accumulation on the mitochondria and Bax-induced permeabilization of the mitochondrial membranes.[23,24]

Our group has identified an antiapoptotic signal activated by the cardiotonic steroid ouabain, which involves interaction between sodium-potassium adenosine triphosphatase (Na,K-ATPase) and the inositol 1,4,5-triphosphate receptor (IP3R) and triggering of slow intracellular calcium oscillations. We have shown that the ouabain signal may interfere with the apoptotic process by down-regulation of the apoptotic factor Bax and up-regulation of the antiapoptotic factor Bcl-xL.[25–30] Studies from us and other investigators

have provided evidence for a tissue protective effect of ouabain.[30–36]

The aim of this study has been to test the hypothesis that activation of the ouabain signal can, via down-regulation of Bax and up-regulation of Bcl-xL, rescue from the onset of albumin-triggered apoptotic process and thereby halt the progression of CKD. If this would be the case, ouabain may be a good candidate for a clinically feasible antiapoptotic drug. Proximal tubular cells (PTCs) are the main target for the toxic effects of albumin overload,[17] and loss of early PTCs will result in glomerular-tubular disconnection and irreversible renal damage.[5,7]

To assess at which stage ouabain interferes with the apoptotic process, Bax recruitment to the mitochondria, changes of the mitochondrial membrane potential, and cellular abundance and localization of Bcl-xL were sequentially studied in a homogenous preparation of primary rat PTCs (RPTCs). Podocytes, which constitute a well-recognized locus minoris resistentiae in CKD,[37,38] were also examined with regard to their apoptotic response to albumin and the rescuing effect of ouabain. To obtain the first proof of principle that ouabain may protect from apoptosis and progressive renal damage in proteinuric CKD, we used a well-established rat model of human proteinuric kidney disease, passive Heymann nephritis (PHN).[39,40]

RESULTS

Albumin uptake into primary renal cells triggers apoptosis followed by increased expression of TGF-β 1: protective effect of ouabain

It is well documented that excessive uptake of albumin into RPTCs triggers apoptosis[30,41–43] and generation of profibrotic factors, such as transforming growth factor (TGF)-β.[44] To determine the order by which these processes are initiated, we incubated RPTCs with fatty acid and endotoxin-free albumin (10 mg/ml) for 2, 4, 8, and 18 hours. The level of apoptosis triggered by albumin was determined with terminal deoxynucleotidyltransferase–mediated dUTP nick end-labeling (TUNEL) staining[45] and expression of the profibrotic TGF-β1 precursor with immunoblotting (Figure 1a–d). Apoptotic index (AI) was significantly increased after 2 hours of albumin incubation and continued to increase during the following 16 hours. In contrast, expression of the TGF-β1 precursor was not increased until after 8 hours of albumin incubation.

The apoptotic effect of albumin was dose-dependent and coincubation with ouabain (5 nM) resulted in a robust reduction of AI with all tested albumin concentrations (5, 10, or 20 mg/ml for 8 or 18 hours) (Figure 1e and f). The expression of TGF-β precursor in RPTCs exposed to albumin for 8 or 18 hours was also attenuated by ouabain (5 nM) (Supplementary Figure S1B). Ouabain did not interfere with albumin uptake in RPTCs (Supplementary Figure S1C).

To test whether albumin might trigger apoptosis of primary rat podocytes, isolated glomeruli were plated, cultured for 3 days, and stained with the podocyte-specific transcriptional factor WT1.[46] AI was determined in cells that had migrated out from the glomerulus and were WT1-positive (Figure 1g). Incubation with albumin for 18 hours triggered apoptosis in a dose-dependent manner. Coincubation with ouabain resulted in significant reduction of AI (Figure 1h).

Ouabain interferes with the albumin triggered intrinsic apoptotic pathway

In RPTCs exposed to albumin (10 mg/ml) for 8 hours, Bcl-xL abundance was decreased and the Bax abundance was increased as measured by immunoblotting (Figure 2b and c). The abundance of cleaved caspase-3 was increased, indicating that the apoptotic process was reaching the point of no return. Ouabain (5 nM) partially rescued from Bcl-xL down-regulation, Bax up-regulation, and increase of cleaved caspase-3.

The ouabain signaling pathway includes activation of the IP3R, release of calcium from endoplasmic reticulum via the IP3R and activation of the prosurvival nuclear factor κB (nuclear factor kappa-light-chain-enhancer of activated B cells) p65 subunit (Figure 2a).[25,27,47] When cells coincubated with albumin and ouabain were depleted of calcium from endoplasmic reticulum stores by sarco/endoplasmic reticulum Ca2+−ATPase pump inhibition with cyclopiazonic acid or coincubated with helenalin, a specific nuclear factor κB p65 subunit inhibitor, the rescuing effects of ouabain were abolished (Figure 2b and c). Ouabain had little effect on Bax and Bcl-xL expression in control cells. The extrinsic apoptotic pathway can be triggered by incubation with lipopolysaccharide. Ouabain (5 nM) did not protect against lipopolysaccharide-triggered cytokine release (Figure 2d, Supplementary Figure S2).

Ouabain protects from albumin-triggered mitochondrial dysfunction

To further characterize the involvement of mitochondria in albumin toxicity, time-sequence studies were performed with regard to mitochondrial membrane potential, Bax colocalization with mitochondria and Bcl-xL abundance (Figure 3a–c). Albumin (2.5 mg/ml) caused time-dependent depolarization of the mitochondrial membrane (Figure 3g). Colocalization between Bax and mitochondria in albumin-exposed cells increased in a time-dependent manner and the increase was significant after 2 hours (Figure 3g). The intensity of the fluorescent signal from Bcl-xL in albumin-incubated RPTCs decreased in a time-dependent manner. Changes were significant after 2 hours of incubation with albumin (Figure 3g). Albumin had no effect on colocalization between Bcl-xL and mitochondria (Supplementary Figure S3A). In RPTCs coincubated with albumin (2.5 mg/ml) and ouabain (5 nM) for 8 hours, the effects on mitochondrial accumulation of Bax, mitochondrial membrane potential, and Bcl-xL abundance were greatly attenuated (Figure 3d–f). Incubation of RPTCs with 10 mg/ml albumin resulted in a more pronounced effect (Supplementary Figure S3B–E) and was seen after 30 minutes (Supplementary Figure S4A–C).

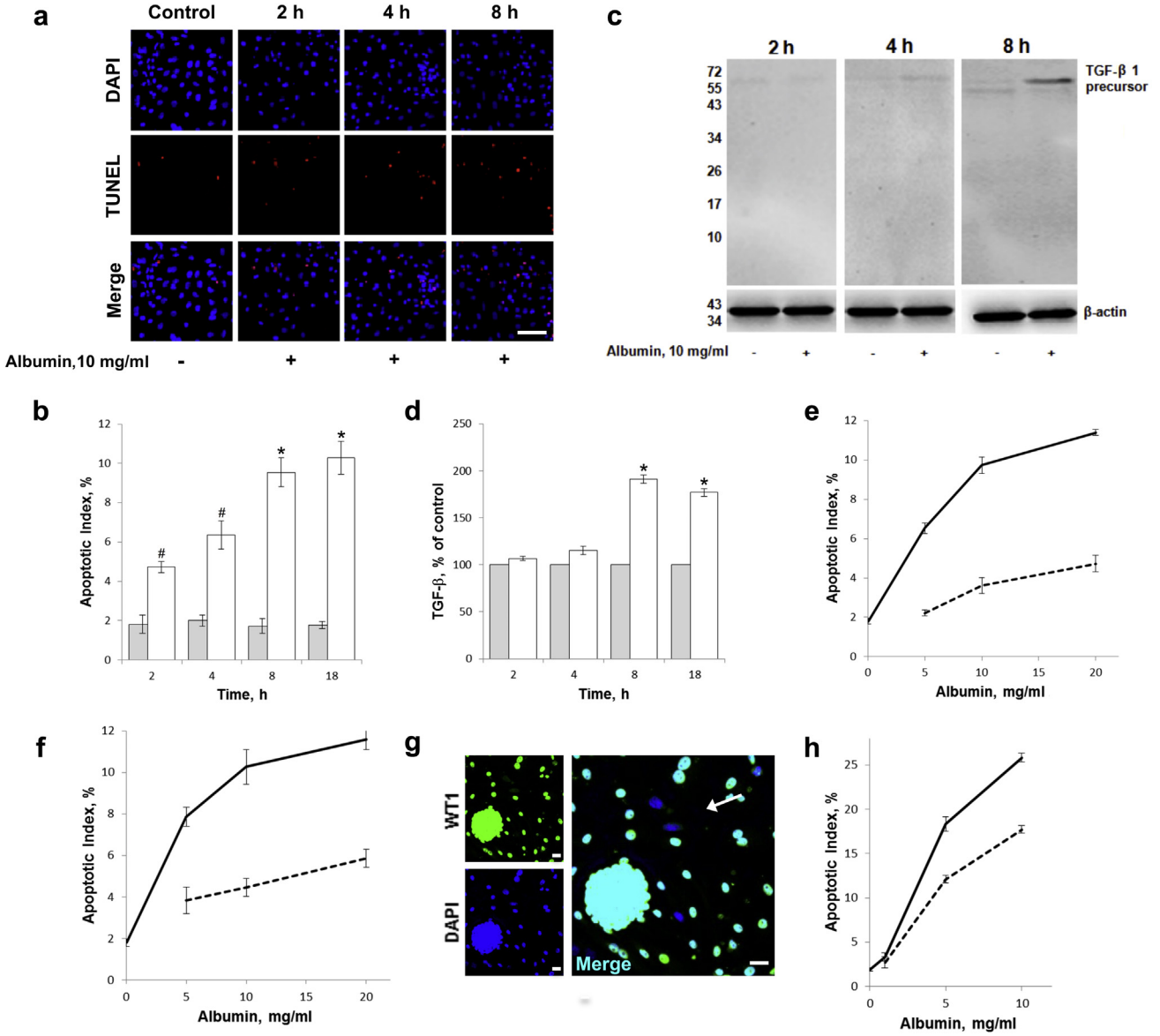

Figure 1 | Albumin uptake into primary renal cells triggers apoptosis followed by increased expression of TGF-β1: protective effect of ouabain. (**a**) Albumin-induced apoptosis in RPTCs incubated with 10 mg/ml albumin for 2, 4, or 8 hours and vehicle control. RPTCs were TUNEL-stained (red) to detect apoptotic cells and counterstained with DAPI (blue). Bar = 40 μm for all images. (**b**) Quantification of albumin-induced apoptosis in RPTCs treated with 10 mg/ml albumin (open bars) or vehicle (gray bars) for 2, 4, 8, or 18 hours. Histograms show mean ± SEM. Experiments were repeated 4 times. The apoptotic index in vehicle-treated (control) cells was stable at 2% for the duration of the 18 hours. The apoptotic index for 10 mg/ml albumin was significantly increased versus control $^{*}P < 0.001$; $^{\#}P < 0.01$. (**c**) Albumin-induced TGF-β1 expression in RPTCs detected by immunoblot. RPTCs were incubated with 10 mg/ml albumin in serum-free medium for 2, 4, or 8 hours. (**d**) Quantification of albumin-induced TGF-β1 expression in RPTCs incubated with 10 mg/ml albumin (open bars) or vehicle (gray bars) for 2, 4, 8, or 18 hours. Experiments were repeated 4 times and vehicle control for each time point was set to 100%. Histograms show mean ± SEM. $^{*}P < 0.001$ versus control. (**e,f**) Dose dependence of albumin-induced apoptosis in RPTCs. RPTCs were incubated with 0 (vehicle control); 5, 10, or 20 mg/ml albumin alone (solid line); and in combination with 5 nM ouabain (dashed line) for 8 hours in **e** or 18 hours in **f**. Plots represent mean ± SEM. Experiments were repeated 4 times. $P < 0.001$ for 5, 10, and 20 mg/ml albumin versus vehicle control (0 mg/ml), at both 8 and 18 hours. $P < 0.01$ for 5 nM ouabain with 5, 10, and 20 mg/ml albumin versus the corresponding albumin treatment alone, at both 8 and 18 hours. (**g**) Primary culture of podocytes; images show isolated rat glomeruli plated and cultured for 3 days. Staining with the podocyte-specific transcriptional factor WT1 shown in green and DAPI-stained nuclei shown in blue. Podocytes that migrate out from the glomerulus were used for the apoptosis study shown in **h**. Note that a subset of cells (indicated by arrow) are not WT1-positive and therefore are not included in the analysis. Bars = 20 μm. (**h**) Dose dependence of albumin-induced apoptosis in podocytes. Podocytes were incubated with 0 (vehicle control); 1, 5, or 10 mg/ml albumin alone (solid line); and in combination with 5 nM ouabain (dashed line) for 18 hours. Only cells positive for the podocyte marker WT1 were included in the analysis. Plots represent mean ± SEM. Experiments were repeated 4 times. $P < 0.001$ for 5 and 10 mg/ml albumin versus vehicle control (0 mg/ml); $P < 0.01$ for ouabain treatment together with 5 and 10 mg/ml albumin versus the corresponding albumin treatment alone. DAPI, 4′,6-diamidino-2-phenylindole; RPTCs, rat proximal tubular cells; TGF, transforming growth factor; TUNEL, terminal deoxynucleotidyltransferase–mediated dUTP nick end-labeling.

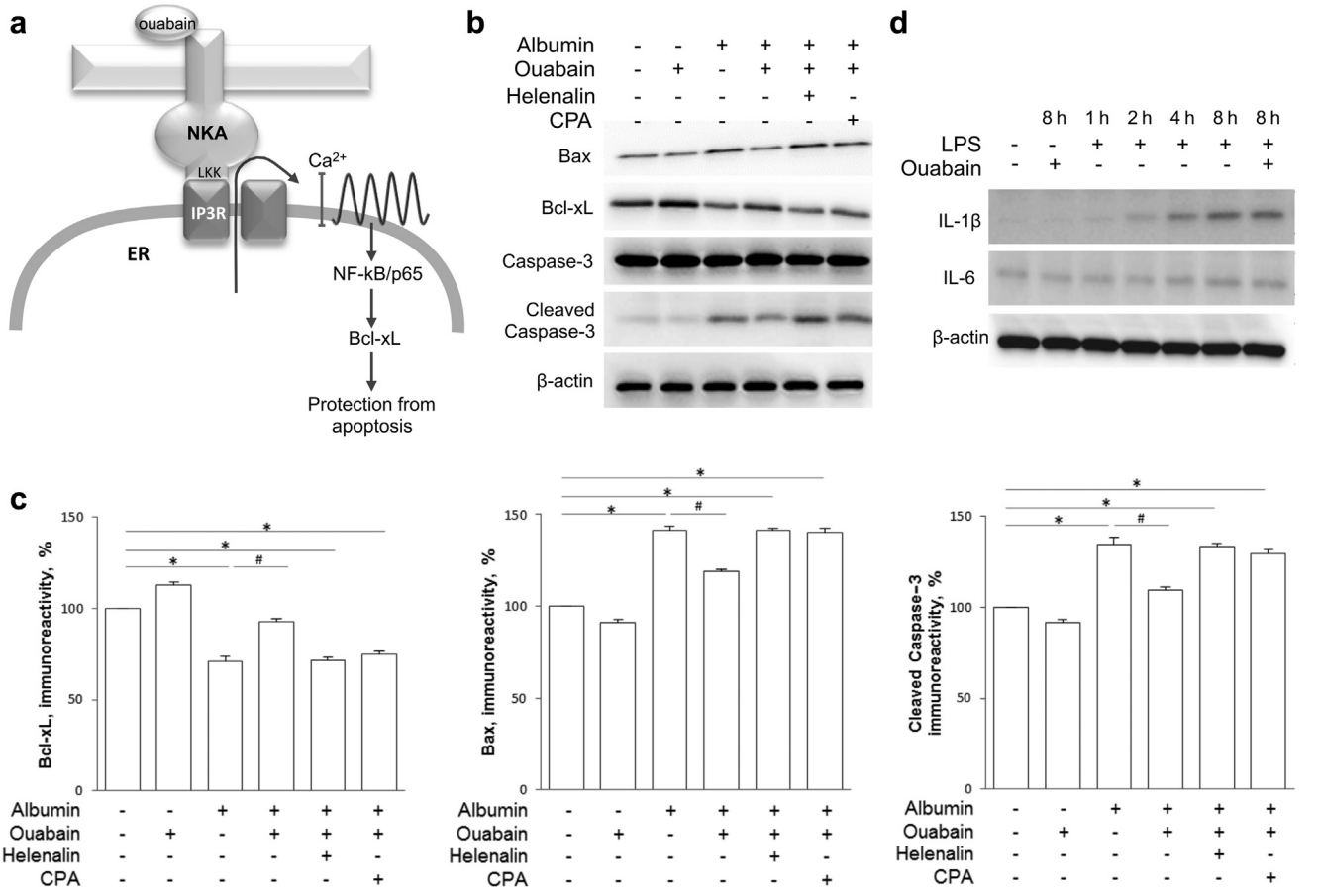

Figure 2 | Ouabain intervenes with the intrinsic apoptotic pathway triggered by albumin, but not with LPS-stimulated cytokine expression. (**a**) Cartoon illustrating the ouabain/Na,K-ATPase/IP3R signaling pathway. Ouabain binds to Na,K-ATPase, which triggers interaction between the Na,K-ATPase and the IP3R through the amino acid residues LKK in the N-terminus of the catalytic α subunit of the Na,K-ATPase. The interaction activates the IP3R, causing calcium to release from the ER. The slow calcium oscillations promote activation the NF-κB p65 subunit, which leads to protection from apoptosis through stimulation of the antiapoptotic protein Bcl-xL. (**b**) Western blot showing expression of Bax, Bcl-xL, caspase-3, and cleaved caspase-3 in RPTCs after 8 hours incubation with 10 mg/ml albumin, 5 nM ouabain, 1 μM Helenalin, and 1μM CPA as indicated. (**c**) Densitometric quantification of Bcl-xL (left), Bax (center), and cleaved caspase-3 (right) after 8 hours incubation with 10 mg/ml albumin, 5 nM ouabain, 1 μM Helenalin, and 1μM CPA as indicated. The density of the band from control cells was set to 100%. Histograms show the mean ± SEM. Experiments were repeated 5 times. $^{*}P < 0.001$; $^{\#}P < 0.01$. (**d**) Expression of the inflammatory cytokines, IL-1β and IL-6, after incubation with LPS 1 μg/ml for 0, 1, 2, 4, or 8 hours, and for 8 hours together with 5 nM ouabain as indicated. Bcl-xL, B-cell lymphoma–extra large; CPA, cyclopiazonic acid; ER, endoplasmic reticulum; IL, interleukin; IP3R, inositol 1,4,5-triphosphate receptor; LPS, lipopolysaccharide; LKK, Leu-Lys-Lys, critical amino acids for NKA and IP3R interaction; NF, nuclear factor; NKA, sodium-potassium adenosine triphosphatase, or Na,K-ATPase; RPTCs, rat proximal tubular cells.

To study whether albumin concentrations in the range of those reported in primary filtrate in proteinuric disease[48] can cause mitochondrial dysfunction, cells were incubated with 0.2 mg/ml albumin. Significant reduction of mitochondrial membrane potential was observed at both 8 and 18 hours. In cells coincubated with ouabain (5 nM) the mitochondrial membrane potential was maintained at control levels (Figure 3h and i).

Chronic ouabain treatment protects from apoptosis in rats with PHN

To assess the nephroprotective effect of ouabain *in vivo*, rats were induced with PHN, a well-studied model of chronic proteinuric kidney disease with a relatively slow progressive course.[39,40] PHN rats were treated with ouabain (15 μg/kg/day) or vehicle and followed for 4 months. Control rats were treated with vehicle. Treatment with this concentration of ouabain does not affect heart rate and arterial pressure (Supplementary Figure S5A). Significant albuminuria was present 2 weeks after PHN induction and was lower in ouabain-treated than in vehicle-treated PHN rats from the fourth week of observation (Supplementary Figure S5B). At the end of the follow-up period, serum creatinine was significantly higher in vehicle-treated than in ouabain-treated PHN rats (Supplementary Figure S5C).

At time of sacrifice, kidneys were prepared for immunohistochemistry and morphometric analysis. Analysis of apoptosis and expression of Bax and Bcl-xL was performed in

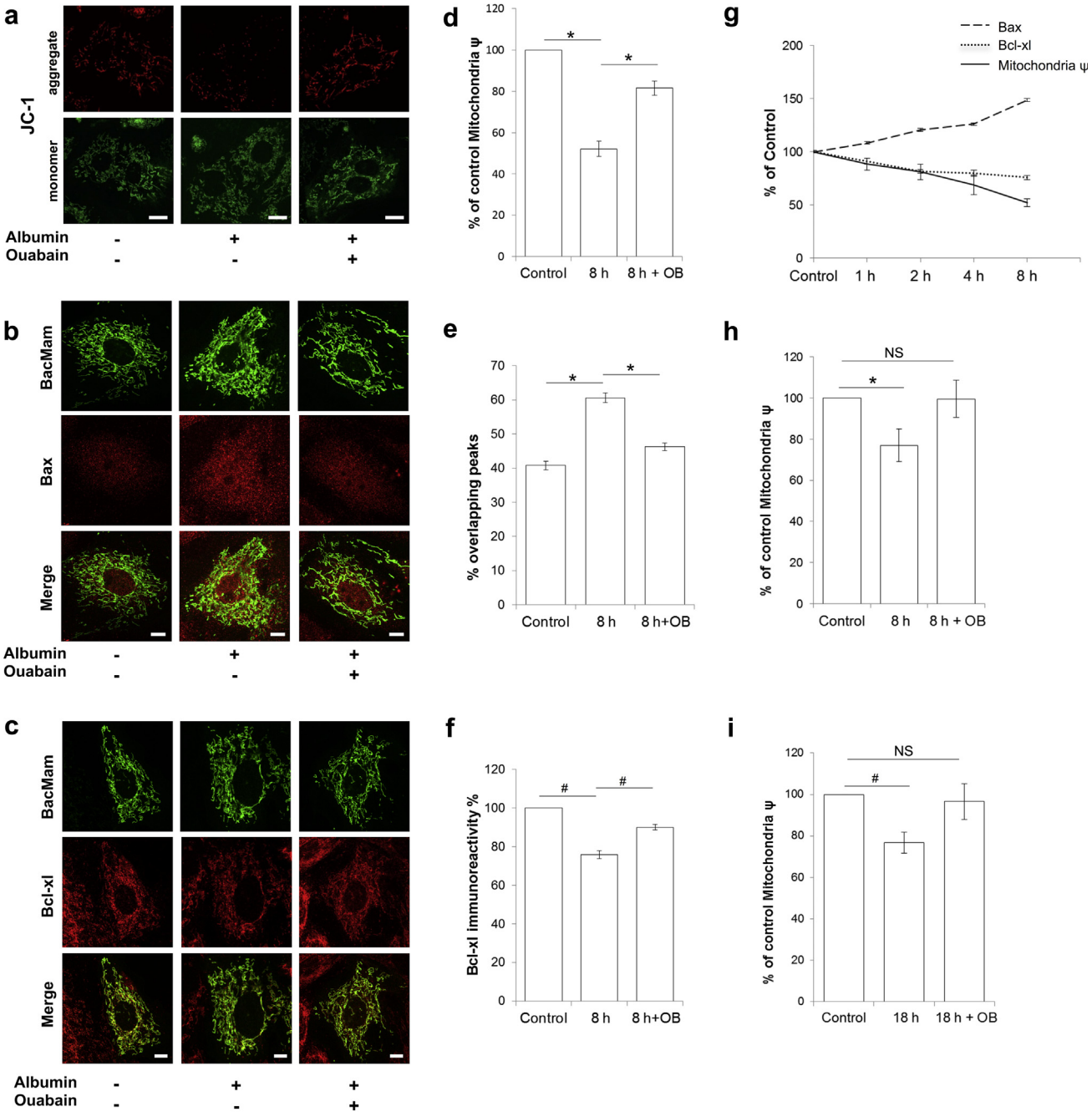

Figure 3 | Ouabain protects from albumin-triggered mitochondrial dysfunction. (**a**) Changes in mitochondrial membrane potential in RPTCs incubated with vehicle, 2.5 mg/ml albumin, or 2.5 mg/ml albumin and 5nM of ouabain for 8 hours, visualized using JC-1 dye. Aggregation of JC-1 indicates high-$\Delta\psi$ mitochondria in red fluorescence. Monomeric dye indicates low-$\Delta\psi$ mitochondria in green fluorescence. Mitochondrial depolarization is shown as a decrease in the red-green fluorescence intensity ratio. Bars = 10 μm. (**b**) Localization of Bax to mitochondria in RPTCs incubated with vehicle, 2.5 mg/ml albumin or 2.5 mg/ml albumin and 5 nM of ouabain for 8 hours. Representative confocal images of Bax immunofluorescence staining shown in red and mitochondria in green, by using the mitochondrial marker BacMam 2.0. Bars = 5 μm. (**c**) Bcl-xL expression in RPTCs incubated with vehicle, 2.5 mg/ml albumin, or 2.5 mg/ml albumin and 5 nM of ouabain for 8 hours. Representative confocal images of Bcl-xL immunofluorescence signal in red and mitochondria in green, by using the mitochondrial marker BacMam 2.0. Bars = 5 μm. (**d**) Quantification mitochondrial membrane potential change in RPTCs incubated with vehicle (control) or 2.5 mg/ml albumin in the presence and absence of 5nM ouabain for 8 hours. $^{*}P < 0.001$. Data are shown as percentage of control, mean ± SEM. Experiments were repeated 3 times. (**e**) Quantification of Bax localization to mitochondria in RPTCs incubated with vehicle (control) or 2.5 mg/ml albumin in the presence and absence of 5 nM ouabain for 8 hours. Colocalization was assessed along 2 perpendicular line traces across the nucleus. Overlap of mitochondria and Bax fluorescence signal peaks along the lines were analyzed. Peaks were considered to overlap if spaced by no more than 140 nm. $^{*}P < 0.001$. Data are shown as percentage of overlapping Bax/mitochondrial peaks, mean ± SEM. Experiments were repeated 4 times. (**f**) Quantification of Bcl-xL expression in RPTCs incubated with vehicle (control) or 2.5 mg/ml albumin in the presence and absence of 5 nM ouabain for 8 hours. $^{\#}P < 0.01$. All data are shown as percentage of Bcl-xL immune reactivity when control was set to

(Continued)

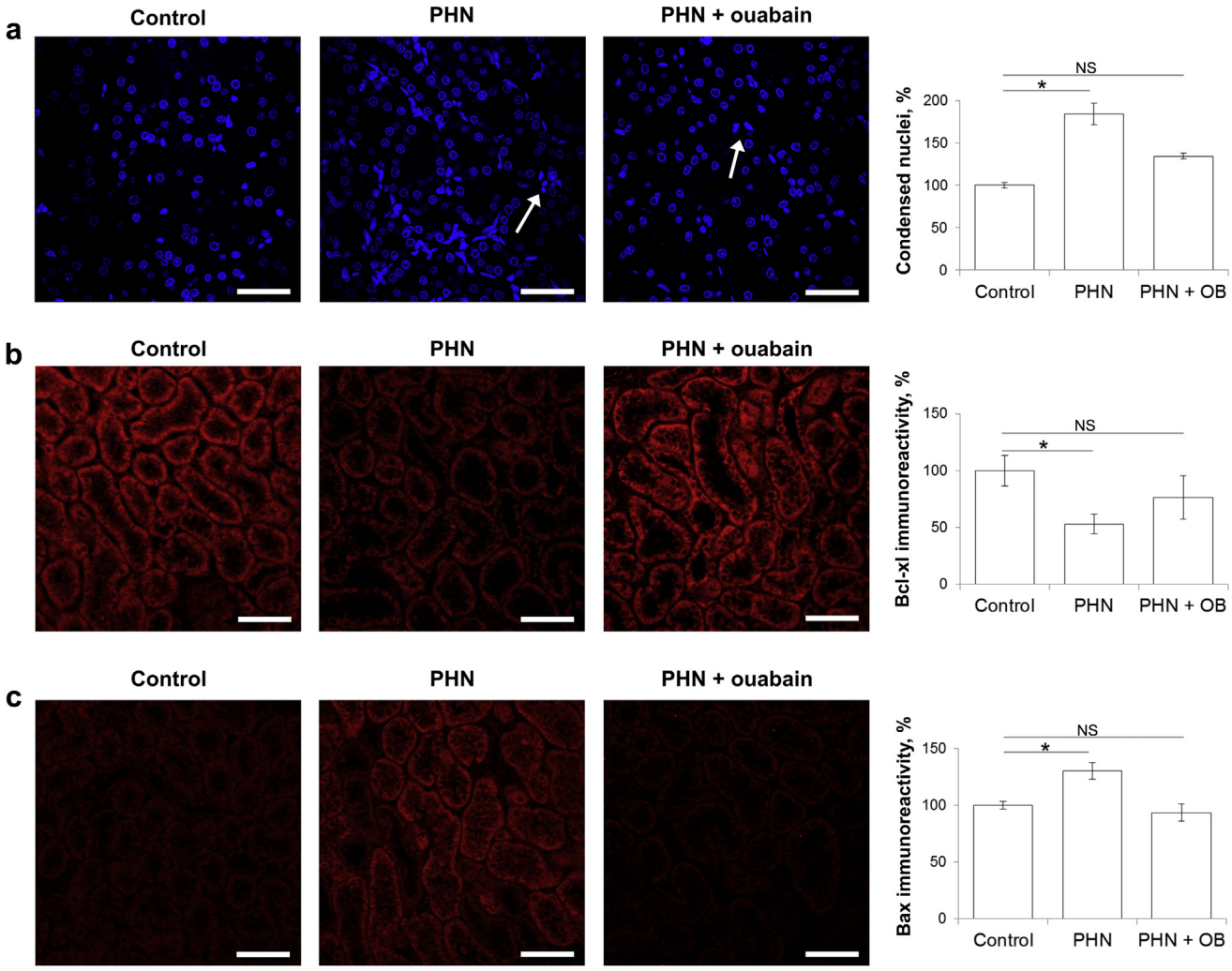

Figure 4 | Long-term treatment with ouabain attenuates apoptosis of renal cortical cells in the PHN rat. (**a**) Representative 4′,6-diamidino-2-phenylindole staining of nuclei in renal cortex of control rats, PHN rats, and ouabain-treated PHN rats at 4 months after PHN induction. The arrows indicate typical condensed nuclei. For quantification, control was set to 100%. Bars = 40 μm. (**b**) Representative immunostaining for Bcl-xL in renal cortex of control rats, PHN rats, and ouabain-treated PHN rats at 4 months after PHN induction. For semiquantitative evaluation of Bcl-xL immunoreactivity signal, control was set to 100%. Bars = 40 μm. (**c**) Representative immunostaining for Bax in renal cortex of control rats, PHN rats, and ouabain-treated PHN rats at 4 months after PHN induction. For semiquantitative evaluation of Bax immunoreactivity signal, control was set to 100%. Bars = 40 μm. For all experiments, analysis was done in 2 sections from each kidney and in 5 (condensed nuclei) or 6 (Bcl-xL and Bax) randomly selected areas of the outer cortex. Histograms show the mean ± SEM. Statistical analysis was performed using analysis of variance followed by Student *t*-test. *$P < 0.05$. Bcl-xL, B-cell lymphoma–extra large; OB, ouabain; PHN, passive Heymann nephritis.

the outer cortex where the vast majority of tubular cells are PTCs,[49] as seen in Supplementary Figure S6. To assess the level of apoptosis, we quantified the number of cells with a condensed (pyknotic) nucleus, a marker of apoptosis that correlate well with TUNEL staining (Supplementary Figure S7). Vehicle-treated PHN animals had a significantly larger number of condensed nuclei than control animals. The number of condensed nuclei in ouabain-treated PHN animals was not different from that of control animals (Figure 4a). Bcl-xL and Bax expression was visualized by immunohistochemistry and semiquantitative evaluation of the fluorescence signal was performed. Renal cortical expression of Bcl-xL and Bax was detected in all groups studied (Figure 4b and c). The Bax immunofluorescence signal was significantly higher and

Figure 3 | (Continued) 100%, mean ± SEM. Experiments were repeated 4 times. (**g**) Plot shows time-dependent change as percentage of control for mitochondrial membrane potential (solid line), localization of Bax to mitochondria (dashed line), and Bcl-xL expression (dotted line) in response to 2.5 mg/ml albumin. (**h,i**) Quantification of mitochondrial membrane potential change in RPTCs incubated with vehicle (control) or 0.2 mg/ml albumin in presence and absence of 5 nM of ouabain for (**h**) 8 hours and (**i**) 18 hours. Data are shown as percentage of control, mean ± SEM. *$P < 0.05$. $^{\#}P < 0.05$. Experiments were repeated 3 times. For all experiments, Mann-Whitney *U* test was used to determine whether differences were statistically significant. Bcl-xL, B-cell lymphoma–extra large; OB, ouabain; RPTCs, rat proximal tubular cells.

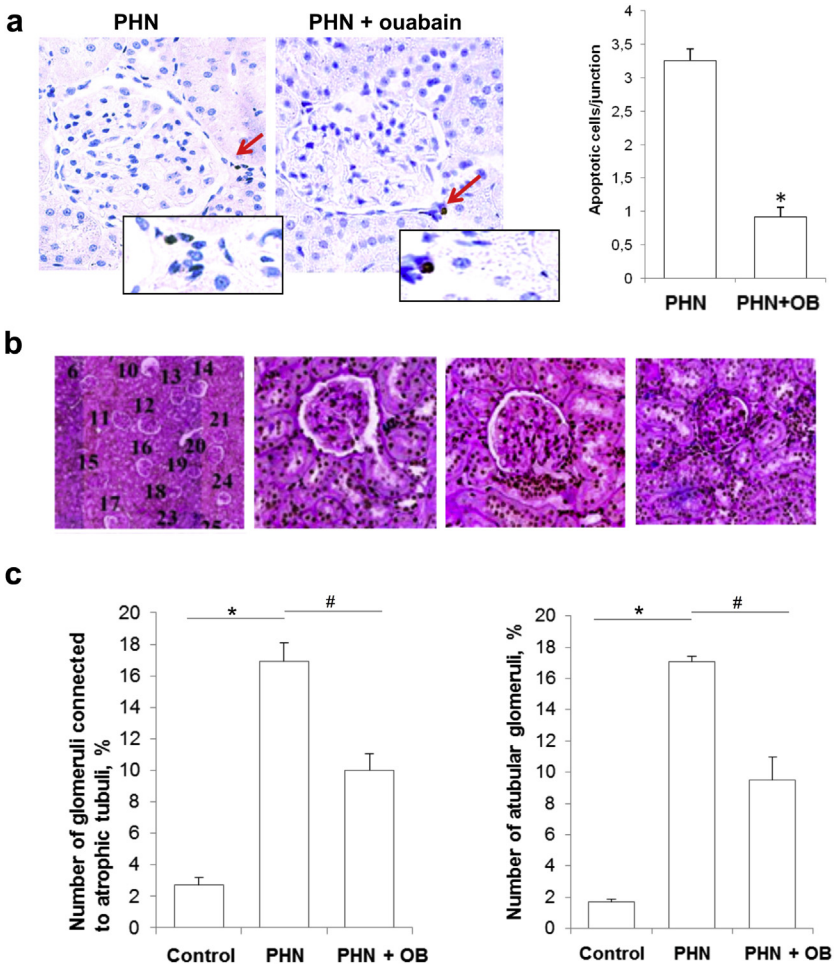

Figure 5 | Kidneys from ouabain-treated PHN rats have fewer disconnected proximal tubules than kidneys from vehicle-treated PHN rats. (**a**) Representative terminal deoxynucleotidyltransferase–mediated dUTP nick end-labeling staining of early proximal tubules from vehicle- and ouabain-treated PHN rats at 4 months after PHN induction. Control rats rarely display any positive terminal deoxynucleotidyl-transferase–mediated dUTP nick end-labeling stain in this region. Histograms show quantitative determination of apoptotic proximal tubular cells, shown as mean ± SEM. $^{*}P < 0.01$. (**b**) Typical periodic acid–Schiff staining of slices for morphometric studies, evaluating the glomerular-tubular connections in individual glomeruli. Pictures illustrate the pattern of glomerular-tubular connections, each glomerulus in the slide is counted (left) and evaluated as connected to a normal proximal tubule (middle left), to an atrophic proximal tubule (middle right), or without a tubular connection, that is, a-tubular glomeruli (right). (**c**) Summary of morphometric studies. Quantitative determination of glomeruli connected to an atrophic proximal tubule (left) and a-tubular glomeruli (right). Histograms represent mean ± SEM. $^{*}P < 0.001$; $^{\#}P < 0.01$. For all experiments, Mann-Whitney *U* test was used to determine significant differences. OB, ouabain; PHN, passive Heymann nephritis.

the Bcl-xL signal was significantly lower in sections from vehicle-treated PHN rats than in sections from control rats. In contrast, neither the Bax nor the Bcl-xL immunofluorescence signal was significantly different between ouabain-treated PHN rats and control rats.

Chronic ouabain treatment protects from glomerular-tubular disconnection in PHN rats

Early PTCs are most exposed to increase in filtered albumin. The number of apoptotic cells at the level of the glomerular-tubular junction was 3-fold higher in kidneys from vehicle-treated than in kidneys from ouabain-treated PHN rats (Figure 5a). Apoptotic cells in the early PTCs were rarely observed in control rats (data not shown).

Apoptosis and atrophy of early PTCs may result in glomerular-tubular disconnection.[7] The frequency of existing and ongoing glomerular-tubular disconnection was studied with morphometric analysis in each animal using on average 75 serial sections (3–4 μm thickness). The number of a-tubular glomeruli and atrophic tubuli were assessed as described by Benigni *et al.*[50] The incidence of a-tubular glomeruli and glomeruli connected to atrophic tubuli was low in control rats. We found a large increase in both a-tubular glomeruli (16%) and glomeruli connected to atrophic tubules (17%) in vehicle-treated PHN rats. The number of a-tubular glomeruli and glomeruli connected to atrophic tubules was significantly less pronounced in ouabain-treated PHN rats (8.5% and 11%, respectively) (Figure 5b and c).

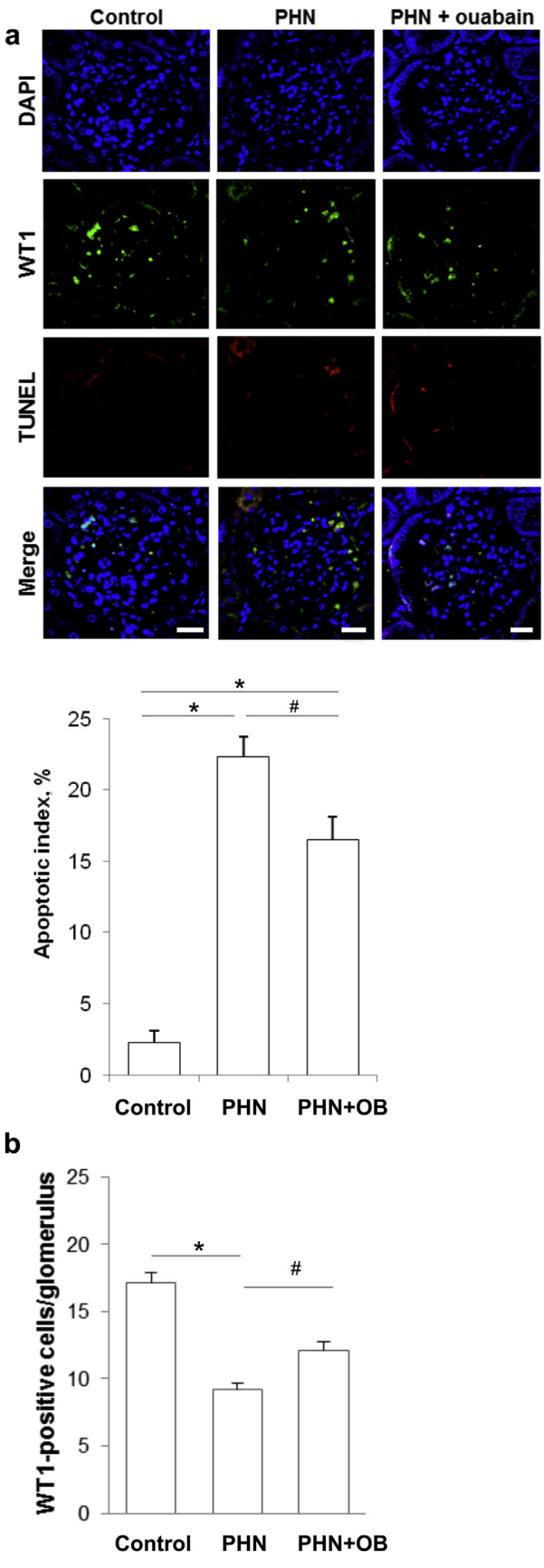

Chronic ouabain treatment protects from loss of podocytes in PHN rats

Loss of podocytes is generally considered a sign of permanent renal damage.[38,51–54] Kidney sections were stained for the podocyte marker WT1. The AI of WT1-positive cells was increased in both vehicle- and ouabain-treated PHN rats, but the increase was significantly less pronounced in ouabain-treated PHN rats (Figure 6a). There was a large reduction of WT1-positive cells per glomerulus in vehicle-treated PHN rats compared with control rats. Significantly more WT1-positive cells were preserved in ouabain-treated PHN animals (Figure 6b).

Kidney fibrosis and glomerular collagen accumulation is less pronounced in ouabain-treated than in vehicle-treated PHN rats

Fibrosis is a typical feature of CKD.[14,16] We found up-regulation of the signal from the profibrotic factor TGF-β1 in vehicle-treated PHN rats compared with control rats. TGF-β1 up-regulation was not observed in ouabain-treated PHN rats (Supplementary Figure S8B). Glomerular collagen IV accumulation was observed in both vehicle- and ouabain-treated PHN rats, but was more pronounced in vehicle-treated PHN rats (Supplementary Figure S8C). Kidneys from adult rats have a regenerative capacity, which may be preserved in CKD.[55,56] Vehicle-treated PHN rats displayed more proliferating cells, detected by markers Ki-67 and proliferating cell nuclear antigen (PCNA), than control rats did. The number of proliferating cells was significantly lower in ouabain-treated than in vehicle-treated PHN rats (Supplementary Figure S8A).

DISCUSSION

The pathogenesis of CKD is multifactorial. Here we confirm the observation from many previous studies that apoptosis contributes to the progressive course of the disease and demonstrate that the progression can be slowed down by ouabain, a compound that acts by interfering with the early phase of the apoptotic process.

There is a great need to develop novel approaches to halt the progression of CKD and specifically target the various

Figure 6 | Kidneys from ouabain-treated PHN rats have more preserved WT1-positive glomerular cells than kidneys from vehicle-treated PHN rats. (**a**) Representative micrographs showing TUNEL stain in WT1-positive glomerular cells from control, vehicle-, and ouabain-treated PHN rats. Sections were TUNEL-stained (red) to detect apoptotic cells and stained for WT1 (green) to detect podocytes; DAPI-stained nuclei are shown in blue. Bars = 20 μm. Histogram shows quantification of apoptotic podocytes, for control, PHN, and ouabain-treated PHN rats. Histograms show mean ± SEM. (**b**) Histogram shows quantification of WT1-positive cells per glomerulus for control, PHN, and ouabain-treated PHN rats. Histograms show mean ± SEM. For all experiments, Mann-Whitney *U* test was used to determine significant differences. $^{*}P < 0.01$; $^{\#}P < 0.05$. DAPI, 4′,6-diamidino-2-phenylindole; OB, ouabain; PHN, passive Heymann nephritis; TUNEL, terminal deoxynucleotidyltransferase–mediated dUTP nick end-labeling.

factors that contribute to the disease process. Although many studies have pointed to the importance of apoptosis in CKD, there is as yet no antiapoptotic drug available. Caspase inhibitors have been tested but have failed to reach the market.[57] Caspase inhibitors interfere with a late stage in the apoptotic pathway and may therefore prevent death of cells where DNA damage has already occurred.

To test whether ouabain protects from the early phase of apoptosis, before the process is irreversible, we focused this study on the effect of ouabain on 2 important members of the Bcl family, the apoptotic protein Bax, and the antiapoptotic protein Bcl-xL. Bax exists in equilibrium between cytosolic and mitochondria-associated forms and shifts toward the latter when activated by a stress stimulus to induce cell death. Activated Bax accumulates on mitochondria and oligomerizes and permeabilizes the mitochondrial outer membrane. This results in release of cytochrome C and marks the point of no return in the apoptotic process. Bcl-xL prevents Bax recruitment to the mitochondria and its oligomerization and permeabilization of the outer mitochondrial membrane. During the course of the apoptotic process, Bax expression increases and Bcl-xL expression decreases. Here we demonstrated that ouabain decreases Bax and increases Bcl-xL expression and that ouabain prevents mitochondrial Bax accumulation and depolarization of the outer mitochondrial membrane in primary PTCs challenged with an excessive load of albumin. These findings indicate that ouabain protects against the onset of albumin-triggered apoptosis. The ouabain effect on the apoptotic pathway is shown in Supplementary Figure S9.

The molecular mechanism by which ouabain exerts its early antiapoptotic effect remains to be elucidated, but it is likely dependent on a signaling pathway involving calcium release from the IP3R. It is possible that ouabain can exert both an acute and a chronic effect. In a previous study,[27] we presented evidence that ouabain may exert a long-term antiapoptotic effect by activating the nuclear factor kB factor p65, a transcriptional regulator of Bcl-xL.[58] Our observation that the Bcl-xL abundance is down-regulated in albumin-triggered cells, maintained in cells treated with ouabain but not in cells treated with ouabain and helenalin, an inhibitor of the transcriptional effects of nuclear factor kB, suggests that this may be the case.

Kidney sections from rats with untreated PHN showed signs of ongoing proximal tubular apoptosis, as indicated by increased Bax and decreased Bcl-xL abundance as well as an elevated number of apoptotic cells. In contrast, a comparison between slices from ouabain-treated PHN rats and control rats did not reveal significant differences with regard to these parameters. A study of the proximal tubules adjacent to the glomeruli showed significantly increased number of apoptotic cells in kidneys from both untreated and ouabain-treated PHN rats as compared to control rats. However, the increase was much more pronounced in untreated than in treated kidneys from PHN rats. Massive apoptosis of early PTCs leads to glomerular-tubular disconnection. Oliver[59] first described the occurrence of a-tubular glomeruli in CKD in 1937. A-tubular glomeruli have more recently been reported in human transplanted kidneys, kidneys from rats with PHN, and in mouse models for obstructive kidney disease and polycystic kidney disease.[39,60–62] Yet glomerular-tubular disconnection has remained an underestimated cause of irreversible loss of renal function in CKD. Notably, the loss of functional nephrons observed in the untreated PHN rats correlated well to the increase in serum creatinine (Supplementary Table S1). Renal tubular cells have a relatively high regenerative capacity.[55,56] The number of newly formed epithelial cells was increased in kidneys from both vehicle- and ouabain-treated PHN rats, but the increase was less pronounced in kidneys from ouabain-treated rats. This regenerative capacity is likely of importance for the preservation of tubular function, but not sufficient to repair a well-advanced or complete glomerular-tubular disconnection.

Excessive exposure to albumin did also trigger apoptosis in primary rat podocytes. Podocytes have low regenerative capacity and the importance of podocyte damage for the progressive course of CKD is well documented. Ouabain protected from podocyte apoptosis both *in vitro* and *in vivo*. The podocyte AI was higher and there were fewer WT1-positive cells per glomeruli in kidneys from untreated than in ouabain-treated PHN rats. PHN is induced by injection of anti-Fx1A antibody, which mainly targets podocyte foot processes. We cannot exclude that complement-dependent cell death may to some extent contribute to podocytes loss. Cell death due to immune reaction, however, is mainly mediated via the extrinsic apoptotic pathway,[63,64] which does not involve Bax and Bcl-xL proteins to the same extent as the mitochondrial apoptotic pathway. It is therefore unlikely that ouabain would have interfered with this pathway.

Tubulointerstitial fibrosis is generally considered as the final common pathway of the majority of progressive CKD.[65,66] Apoptosis is regularly observed in fibrotic tissue, and mounting evidence suggest that apoptosis contributes to the fibrotic process.[31,67–69] It was recently reported that expression of reticulon 1, a protein that induces apoptosis, attenuates the fibrotic process and the severity and progression of CKD in mice and humans.[70] In the albumin exposed PTCs, apoptosis preceded the increase in expression of the multifunctional protein TGF-β, which triggers formation of extracellular matrix and fibrosis as well as apoptosis (likely via the extrinsic apoptotic pathway).[71] Ouabain down-regulated TGFβ expression, both in the *in vitro* and *in vivo* studies, suggesting that execution of apoptosis via the intrinsic mitochondrial pathway precedes the increased TGFβ expression. Taken together, available information indicates that a drug targeting the onset of the mitochondrial apoptotic pathway should be highly beneficial in CKD.

A large number of studies performed on rodents have suggested that albumin is a major contributor to the progressive course of CKD. Yet many patients with minimal change disease or membranous glomerular nephritis can have stable nephrotic-range proteinuria for many years without apparent loss of renal function. However, these observations are not necessarily contradictory. Most patients with minimal change disease are very young, and it is well documented that the regenerative capacity of renal tubular cells is age-dependent and younger patients have a more favorable prognosis than older patients do.[72,73] It is also important to consider that the progression of CKD to renal failure is generally a slow process[3] that often takes more than a decade, and most patients are relatively asymptomatic as long as 50% of the renal functional capacity is preserved. Currently, kidney biopsy specimens from humans are rarely examined for apoptosis and expression of pro-apoptotic proteins. More information about the incidence of apoptosis in human kidneys would likely increase the awareness that clinically relevant drugs targeting the apoptotic process before the point of no return would be beneficial.

In conclusion, this study highlights apoptosis as a cause of albumin toxicity and as a contributor to the progressive loss of functional renal tissue in CKD, and it provides a basis for the development of the cardiotonic steroid ouabain as a complementary therapy in CKD.

MATERIALS AND METHODS

The complete materials and methods including a list of antibodies used can be found in Supplementary Material.

Animals and rat primary cultures

Forty-day-old male Sprague-Dawley rats were used for the PHN model. For cell preparation, 20-day-old male Sprague-Dawley rats were used. All experiments were performed according to Karolinska Institutet regulations concerning care and use of laboratory animals and were approved by the Stockholm North Ethical Evaluation Board for Animal Research.

Primary culture of RPTCs was prepared as previously described.[74] Characterization of RPTCs show that on day 3 in culture 99% of the cells express sodium glucose transport-2 (SGLT-2), a marker for proximal tubular cells (Supplementary Figure S1A). Glomeruli isolation and podocytes culture were performed as previously described.[75] Albumin treatment of primary cultures was started on day 2 or 3 *in vitro* for all experiments, cells were exposed either vehicle (phosphate-buffered saline) or fatty acid and endotoxin-free bovine albumin in the growth media for up to 18 hours, with or without presence of ouabain 5 nM.

Detection of apoptosis in primary culture

TUNEL assay by use of ApopTag Red In Situ Apoptosis Detection kit (Merck Millipore, Billerica, MA) was used according to the manufacturer's instructions. Nuclei were counterstained with 4′,6-diamidino-2-phenylindole (DAPI). For determination of AI in podocytes, podocytes were detected by anti-WT1 antibody.

Mitochondrial membrane potential determination

The integrity of the mitochondrial membrane potential was measured in RPTCs using the JC-1 dye (Life Technologies, Thermo Fisher Scientific, Carlsbad, CA). Mitochondrial depolarization is detected by a shift in fluorescence emission from red (~590 nm) to green (~527 nm). Cells were incubated with 2.5 μg/ml JC-1 dye in cultured medium for 15 minutes at 37 °C and then analyzed. The mitochondrial membrane potential change was quantified by calculating the ratio of red to green fluorescence intensity.

Immunocytochemistry

RPTCs and podocytes in primary culture were fixed in 4% paraformaldehyde for 10 minutes, washed and treated with 0.3% Triton X-100 for 10 minutes. Then incubated with 5% bovine serum albumin, 0.1% Triton X-100, for 1 hour. Primary antibodies were applied overnight at 4 °C. Following 3 washes, cells were incubated with secondary antibodies for 1 hour at room temperature. Cells were washed and mounted for analysis.

Bax, Bcl-xL translocation assessment

RPTCs on day 2 *in vitro* were labeled with CellLight Mitochondria-GFP BacMam (Life Technologies) overnight. The following day, RPTCs were incubated with albumin with or without ouabain or vehicle for up to 8 hours. Following incubation, cells were immunostained for Bax or Bcl-xL, and analysis of Bax/Bcl-xL translocation to the mitochondria was done. To assess colocalization between immune-labeled Bax/Bcl-xL and green fluorescent protein–expressing mitochondria, the method of Edlich *et al.* (2011)[23] was used. Results are shown as fraction of Bax/Bcl-xL—mitochondria overlap to total number of mitochondria.

Animal model, passive Heymann nephritis

Animals were divided into a control group and a PHN group. PHN was induced by a single injection of rabbit anti-Fx1A antibody (a kind gift from Professor David J. Salant, Boston University Medical Center), control rats were given vehicle. On day 0 after PHN injection, one-half of the group was started on ouabain treatment (15 μg/ml/day) and the other half was given vehicle (sterile phosphate-buffered saline) delivered by minipumps implanted subcutaneously. All animals were followed for 4 months. Spot urine samples were collected every second week and albuminuria was measured using Nephrat II (Exocell, Philadelphia, PA). At killing, blood samples were collected for serum creatinine determination and kidneys were removed from for histological and morphological studies.

Renal histology and morphometric analysis

Dissected kidneys were fixed in Dubosq-Brazil, dehydrated in alcohol, and embedded in paraffin. Kidney sections 3 to 4 μm were stained with periodic acid–Schiff reagent, and sections including superficial and juxtamedullary glomeruli were evaluated.

To assess glomerular-tubular disconnection, on average, 75 serial sections (3–4 μm) were examined for each animal. For each group of animals, 300 to 320 glomeruli were examined. Only glomeruli located entirely within the serially sectioned tissue were included in the analysis. The glomeruli were classified as connected to a normal proximal tubule, connected to an atrophic proximal tubule, or without a tubular connection.

Detection of apoptosis in renal tissue

To detect apoptotic PTCs, kidney sections were deparaffinized, rehydrated, and subjected to antigen retrieval, and nuclei were stained with DAPI and sections mounted with Immu-Mount (Thermo Fisher Scientific, Kalamazoo, MI). All samples were stained under identical conditions and analyzed using identical microscopy settings. Cells were classified as being apoptotic if they had a condensed nucleus, where the nuclei was shrunken and had abnormal morphology with no visible interior.

To detect apoptotic podocytes, sections were consecutively immunostained using WT1 antibodies, a podocyte marker, followed by ApopTag Red In Situ Apoptosis Detection kit according to the manufacturer's instructions.

To evaluate apoptotic PTCs at the level of the glomerular-tubular junction, sections were stained with Peroxidase In Situ Apoptosis Detection kit (Merck Millipore) according to manufacturer's instructions and counterstained with Harris hematoxylin (Richard Allan Scientific, Thermo Fisher Scientific). Sections were assessed and the number of apoptotic cells per glomerular-tubular junction was determined. In each slice, 25 to 30 randomly selected glomeruli were examined.

Statistical analysis

Results are presented as mean ± SEM. To determine differences among groups, 2-way analysis of variance followed by Fisher-LSD *post hoc* test was used. If the distribution of the variables was not parametric, the nonparametric Mann-Whitney test was used. Comparisons between groups were made using Kruskal-Wallis 1-way analysis of variance on ranks with pair-wise multiple comparisons made by Dunn method.

DISCLOSURE

All the authors declared no competing interests.

ACKNOWLEDGMENTS

This study was supported by the Swedish Research Council and the Erling-Persson Family Foundation to AA and the Karolinska Institutet KIRT fellowship to EB. The authors wish to thank Dr. Tommy Linné, Karolinska Institutet, for valuable advice and Kristoffer Bernhem, Karolinska Institutet, for assistance with data analysis. Parts of this work have been presented at the 2014 American Society of Nephrology meeting. This work was also presented by AA as part of the 2015 Hugh Davson Distinguished Lectureship of the Cell and Molecular Physiology Section at the Experimental Biology meeting in Boston 2015.

SUPPLEMENTARY MATERIAL

Supplementary Materials and Methods

Figure S1. Rat proximal tubule cells in culture: maintenance of fenotype, TGF-β1 response to albumin uptake, and lack of ouabain effect on albumin uptake. (**A**) Characterization of RPTCs. RPTCs on day 3, 6, and 10 in culture were immunostained for SGLT-2 (green), a marker of proximal tubule cells, and for alpha-smooth muscle actin (red), a marker of fibroblasts, and DAPI (blue) to count the total number of cells. At day 3, 99% of the cells express SGLT-2 and 1% expressed alpha-smooth muscle actin. At day 6, 75% and at day 10, 46% of the cells were SGLT-2–positive and alpha-smooth muscle actin–negative. In addition, at day 6, 25% and at day 10, 53% express both SGLT-2 and alpha-smooth muscle actin. (**B**) TGF-β1 expression detected by immunoblotting in RPTCs incubated with or without 10 mg/ml albumin and in combination with ouabain 5 nM for 8 or 18 hours. Histograms show quantification of albumin-induced TGF-β1 expression data are mean ± SEM. $^{**}P < 0.001$; $^{*}P < 0.01$. Experiments were repeated 4 times. (**C**) Ouabain does not influence RPTCs albumin uptake. RPTCs incubated with 2.5 mg/ml albumin and 10 μl/ml Alexa 555 albumin with or without 5 nM ouabain for 2 hours. Histograms show quantification of Alexa 555 albumin signal per cell. Data are shown as mean ± SEM. Experiments were repeated 6 times. DAPI, 4′,6-diamidino-2-phenylindole; RPTCs, rat proximal tubular cells; SGLT-2, sodium glucose transporter-2; TGF, transforming growth factor.

Figure S2. Ouabain does not inhibit LPS stimulated cytokine expression. Quantification of expression of the inflammatory cytokines, IL-1β (top) and IL-6 (bottom), after incubation with LPS 1μg/ml for 0, 1, 2, 4, or 8 hours, and for 8 hours together with 5 nM ouabain. Experiments were repeated 3 times. Data are mean ± SEM, $^{**}P < 0.001$; $^{*}P<0.01$. IL, interleukin; LPS, lipopolysaccharide.

Figure S3. Time-dependent effects of early apoptotic signs triggered by 10 mg/ml albumin exposure. (**A**) Quantification of Bcl-xL localization to mitochondria in RPTCs incubated with 2.5 mg/ml (open bars) and 10 mg/ml (gray bars) albumin for 8 hours in presence and absence of 5 nM ouabain. All data are shown as percentage of overlapping Bcl-xl/mitochondrial peaks, mean ± SEM. Experiments were repeated 4 times. (**B**) Plot shows time-dependent change as percentage of control for mitochondrial membrane potential (solid line), localization of Bax to mitochondria (broken line), and Bcl-xL expression (dotted line) in RPTCs exposed to 10 mg/ml albumin. (**C**) Quantification of mitochondrial membrane potential change in RPTCs incubated with vehicle (control) or 10 mg/ml albumin in presence and absence of 5nM of ouabain for 8 hours. $^{*}P < 0.001$; $^{\#}P < 0.01$. Data are shown as percentage of control, mean ± SEM. Experiments were repeated 3 times. (**D**) Quantification of Bax localization to mitochondria in RPTCs incubated with vehicle (control) or 10 mg/ml albumin in presence and absence of 5 nM of ouabain for 8 hours. $^{*}P < 0.001$; $^{\#}P < 0.01$. Data are shown as percentage of overlapping Bax/mitochondrial peaks, mean ± SEM. Experiments were repeated 4 times. (**E**) Quantification of Bcl-xL expression in RPTCs incubated with vehicle (control) or 10 mg/ml albumin in presence and absence of 5 nM of ouabain for 8 hours. $^{*}P < 0.001$; $^{\#}P < 0.01$. Data are shown as percentage of Bcl-xL immune reactivity when control was set to 100%, mean ± SEM. Experiments were repeated 4 times. Bcl-xL, B-cell lymphoma–extra large; OB, ouabain; RPTCs, rat proximal tubular cells.

Figure S4. Initial effects of 10 mg/ml albumin exposure of proximal tubular cells on Bax expression and mitochondrial membrane potential. (**A**) Albumin uptake, RPTCs were incubated with 10 mg/ml albumin and trace Alexa 555 coupled albumin for 5, 15, 30, and 45 minutes. All images represent a single section through the focal plane. (**B**) Localization of Bax to mitochondria in RPTCs incubated with 10 mg/ml albumin for 5, 15, 30, and 45 minutes. Bax immunofluorescence staining is shown in red and mitochondria in green, by using the mitochondrial marker BacMam 2.0. Histograms show percentage of overlapping Bax/mitochondrial peaks, mean ± SEM. Experiments were repeated 3 times. $^{*}P < 0.05$ and $^{**}P < 0.01$ versus control rats. (**C**) Mitochondrial membrane potential change in RPTCs incubated with albumin 10 mg/ml for 5, 15, 30, and 45 minutes. Mitochondrial membrane potential change was visualized using JC-1 dye; green shows depolarized membrane, red shows polarized membrane. Histograms show percentage of control, mean ± SEM. Experiments were repeated 3 times. $^{**}P < 0.01$ versus control. RPTCs, rat proximal tubular cells.

Figure S5. Blood pressure, albumin excretion, and serum creatinine in vehicle- and ouabain-treated control and PHN rats. (**A**) Heart rate in mm Hg (left) and blood pressure in bpm (right) for vehicle- and ouabain- treated (15 μg/kg/day) rats during 8 weeks.

Measurements were performed on unanesthetized rats using tail cuff. Data are mean ± SEM. (**B**) Urinary albumin/creatinine levels in control, vehicle-, and ouabain-treated (15 μg/kg/day) PHN rats during 16 weeks. Data are mean ± SEM. $^{*}P < 0.05$ for control versus PHN and control versus PHN + ouabain at 2 weeks. $^{\#}P < 0.05$ for control versus PHN, control versus PHN + ouabain, and PHN versus PHN + ouabain at the corresponding time points. For all experiments, statistical analysis was performed using 2-way analysis of variance. (**C**) Serum creatinine levels (mg/dl) in control, vehicle-, and ouabain-treated (15 μg/kg/day) PHN rats at experiment end point at 16 weeks. Histograms show the mean ± SEM. The Mann-Whitney *U* test was used to determine whether differences were statistically significant. $^{**}P < 0.001$; $^{*}P < 0.01$. bpm, beats per minute; OB, ouabain; PHN, passive Heymann nephritis.

Figure S6. Identification of proximal tubular cells in kidney sections. Analysis of apoptosis by condensed nuclei, expression of Bax and Bcl-xL done in control, PHN, and ouabain-treated PHN rats as presented in Figure 4 was performed exclusively in the outer cortical layer. The majority of tubules in the cortical area (left image) are proximal tubules as verified by immunostaining for SGLT-2 (green) used as a specific marker of proximal tubule cells. In comparison, an area closer to the center of the kidney slice has few or no proximal tubules as shown by the absence of SGLT-2 staining (right image). DAPI staining of nuclei is shown in blue. Bars = 40 μm. DAPI, 4′,6-diamidino-2-phenylindole; PHN, passive Heymann nephritis; SGLT-2, sodium glucose transporter-2.

Figure S7. Comparison of condensed nuclei and TUNEL methods for assessment of apoptosis. RPTCs on the same coverslip were analyzed using both condensed nuclei and TUNEL. Studies were performed on control RPTCs and RPTCs exposed to 2.5 to 10 mg/ml albumin for 8 hours. The plot (left) shows the percentage of apoptosis expressed by condensed nuclei and by TUNEL for each coverslip analyzed. There is a linear correlation between the 2 methods, $y = 0.9944x$ and $R^2 = 0.7339$. The table (right) shows the average percentage of apoptosis for each treatment assessed with condensed nuclei and with TUNEL. RPTCs, rat proximal tubular cells; TUNEL, terminal deoxynucleotidyltransferase–mediated dUTP nick end-labeling.

Figure S8. Cell proliferation, TGF-β1 expression, and glomerular collagen in kidney sections from PHN rats. (**A**) Quantification of proliferative markers Ki-67 and PCNA from immunohistochemistry in kidney sections from control, PHN, and ouabain-treated PHN rats. Histograms show mean ± SEM. Mann-Whitney *U* test was used to determine significant differences. $^{**}P < 0.001$. (**B**) Representative expression of profibrotic factor TGF-β1 (red) and nuclei (DAPI, blue) in control, vehicle-treated PHN, and ouabain-treated PHN rats. Semi-quantitative evaluation of the TGF-β1 signal was performed in section from control, vehicle-treated PHN, and ouabain-treated PHN animals, and 3 areas corresponding to 75% of the cortex were analyzed. Immunoreactivity for TGF-β1 is expressed as percentage of deviation from control. Histograms show mean ± SEM. Statistical analysis was performed using the Mann-Whitney *U* test. $^{**}P < 0.001$. (**C**) Representative images of collage IV immunostaining in glomeruli of control, vehicle-treated, and ouabain-treated PHN rats. The images are representative. Level of collagen IV in control animals was set to baseline and data are expressed as percentage increase from control. Histograms show mean ± SEM. Statistical analysis was performed using the Mann-Whitney *U* test. $^{*}P < 0.05$ DAPI, 4′,6-diamidino-2-phenylindole; PCNA, proliferating cell nuclear antigen; PHN, passive Heymann nephritis; TGF, transforming growth factor.

Figure S9. Ouabain rescues from albumin triggered apoptosis before the point of no return. The intrinsic mitochondrial apoptotic program is controlled by the Bcl-2 family of apoptotic and antiapoptotic proteins. Bcl-xL is a prominent member of the antiapoptotic Bcl-2 proteins, and Bax is a prominent member of the apoptotic Bcl-2 proteins. Under control conditions, Bax is mainly located in the cytosol and Bcl-xL on the mitochondria. Apoptosis is initiated by the restructuring of Bax and its translocation to the mitochondria. Bcl-xL acts by retranslocating Bax to the cytosol. Accumulation of Bax on the mitochondria promotes its homo-oligomerization as well as its hetero-oligomerization with other apoptotic proteins.[24,76] This results in permeabilization of the mitochondrial membrane and leakage of cytochrome C, which marks the point of no return in the apoptotic process. During the course of the apoptotic process, the abundance of Bax increases and the abundance of Bcl-xL decreases. Ouabain acts by protecting from the accumulation of Bax on the mitochondrial membrane as well as from up-regulation of Bax and down-regulation of Bcl-xL abundance. Bcl-xL, B-cell lymphoma–extra large.

Table S1. Correlation between atrophic/loss of glomerular tubular junction and serum creatinine in control and PHN rats. OB, ouabain; PHN, passive Heymann nephritis.

Supplementary material is linked to the online version of the paper at www.kidney-international.org.

REFERENCES

1. United States Renal Data System. *USRDS 2013 Annual Data Report: Atlas of Chronic Kidney Disease and End-Stage Renal Disease in the United States*. Bethesda, MD: National Institutes of Health, National Institute of Diabetes and Digestive and Kidney Diseases; 2013.
2. Anderson S, Halter JB, Hazzard WR, et al, for the High KP, Workshop Participants. Prediction, progression, and outcomes of chronic kidney disease in older adults. *J Am Soc Nephrol*. 2009;20:1199–1209.
3. Inker LA, Lambers Heerspink HJ, Mondal H, et al. GFR decline as an alternative end point to kidney failure in clinical trials: a meta-analysis of treatment effects from 37 randomized trials. *Am J Kidney Dis*. 2014;64:848–859.
4. Haraldsson B, Nyström J, Deen WM. Properties of the glomerular barrier and mechanisms of proteinuria. *Physiol Rev*. 2008;88:451–487.
5. Remuzzi G, Perico N, Macia M, Ruggenenti P. The role of renin-angiotensin-aldosterone system in the progression of chronic kidney disease. *Kidney Int Suppl*. 2005;99:S57–65.
6. Chevalier RL, Forbes MS. Generation and evolution of atubular glomeruli in the progression of renal disorders. *J Am Soc Nephrol*. 2008;19:197–206.
7. Lindop GB, Gibson IW, Downie TT, et al. The glomerulo-tubular junction: a target in renal diseases. *J Pathol*. 2002;197:1–3.
8. Fukuda A, Wickman LT, Venkatareddy M, et al. Progression is caused by angiotensin II-dependent persistent podocytes loss from destabilized glomeruli. *Kidney Int*. 2012;81:40–55.
9. Weening JJ, Ronco P, Remuzzi G. Advances in the pathology of glomerular diseases. *Contrib Nephrol*. 2013;181:12–21.
10. Tojo A, Kinugasa S. Mechanisms of glomerular albumin filtration and tubular reabsorption. *Int J Nephrol*. 2012;2012:481520.
11. Perkins BA, Ficociello LH, Ostrander BE, et al. Microalbuminuria and the risk for early progressive renal function decline in type 1 diabetes. *J Am Soc Nephrol*. 2007;18:1353–1361.
12. Zoja C, Abbate M, Remuzzi G. Progression of renal injury toward interstitial inflammation and glomerular sclerosis is dependent on abnormal protein filtration. *Nephrol Dial Transplant*. 2015;30:706–712.
13. Birn H, Christensen EI. Renal albumin absorption in physiology. *Kidney Int*. 2006;69:440–449.
14. Brezniceanu M-L, Liu F, Wei C-C, et al. Attenuation of interstitial fibrosis and tubular apoptosis in db/db transgenic mice overexpressing catalase in renal proximal tubular cells. *Diabetes*. 2008;57:451–459.
15. Sanz AB, Santamaría B, Ruiz-Ortega M, et al. Mechanisms of renal apoptosis in health and disease. *J Am Soc Nephrol*. 2008;19:1634–1642.
16. Eddy AA. Molecular basis of renal fibrosis. *Pediatr Nephrol*. 2000;15:290–301.

17. Erkan E, Devarajan P, Schwartz GJ. Mitochondria are the major targets in albumin-induced apoptosis in proximal tubule cells. *J Am Soc Nephrol*. 2007;18:1199–1208.
18. Erkan E, Garcia CD, Patterson LT, et al. Induction of renal tubular cell apoptosis in focal segmental glomerulosclerosis: roles of proteinuria and Fas-dependent pathways. *J Am Soc Nephrol*. 2005;16:398–407.
19. Jafar TH, Stark PC, Schmid CH, et al, for the AIPRD Study Group. The effect of angiotensin-converting-enzyme inhibitors on progression of advanced polycystic kidney disease. *Kidney Int*. 2005;67:265–271.
20. Essien E, Goel N, Melamed ML. Role of vitamin D receptor activation in racial disparities in kidney disease outcomes. *Semin Nephrol*. 2013;33:416–424.
21. Akhurst RJ, Hata A. Targeting the TGFβ signaling pathway in disease. *Nat Rev Drug Discov*. 2012;11:790–811.
22. de Zeeuw D, Agarwal R, Amdahl M, et al. Selective vitamin D receptor activation with paricalcitol for reduction of albuminuria in patients with type 2 diabetes (VITAL study): a randomised controlled trial. *Lancet*. 2010;376:1543–1551.
23. Edlich F, Banerjee S, Suzuki M, et al. Bcl-x(L) retrotranslocates Bax from the mitochondria into the cytosol. *Cell*. 2011;145:104–116.
24. Chen HC, Kanai M, Inoue-Yamauchi A, et al. An interconnected hierarchical model of cell death regulation by the BCL-2 family. *Nat Cell Biol*. 2015;17:1270–1281.
25. Miyakawa-Naito A, Uhlen P, Lal M, et al. Cell signaling microdomain with Na,K-ATPase and inositol 1,4,5-trisphosphate receptor generates calcium oscillations. *J Biol Chem*. 2003;278:50355–50361.
26. Aizman O, Uhlen P, Lal M, et al. Ouabain, a steroid hormone that signals with slow calcium oscillations. *Proc Natl Acad Sci U S A*. 2001;98:13420–13424.
27. Li J, Zelenin S, Aperia A, Aizman O. Low doses of ouabain protect from serum deprivation–triggered apoptosis and stimulate kidney cell proliferation via activation of NF-kappaB. *J Am Soc Nephrol*. 2006;17:1848–1857.
28. Fontana JM, Burlaka I, Khodus G, et al. Calcium oscillations triggered by cardiotonic steroids. *FEBS J*. 2013;280:5450–5455.
29. Aperia A. 2011 Homer Smith Award: to serve and protect: classic and novel roles for Na+, K+-adenosine triphosphatase. *J Am Soc Nephrol*. 2012;23:1283–1290.
30. Burlaka I, Liu XL, Rebetz J, et al. Ouabain protects from Shiga toxin-triggered apoptosis by reversing the imbalance between Bax and Bcl-xL. *J Am Soc Nephrol*. 2013;24:1413–1423.
31. Aperia AC, Akkuratov EE, Fontana JM, Brismar H. Na^+, K^+-ATPase, a new class of plasma membrane receptors. *Am J Physiol Cell Physiol*. 2016;310:C491–495.
32. Dvela-Levitt M, Cohen-Ben Ami H, Rosen H, et al. Reduction in maternal circulating ouabain impair offspring growth and kidney development. *J Am Soc Nephrol*. 2015;26:1103–1114.
33. Jacobs BE, Liu Y, Pulina MV, et al. Normal pregnancy: mechanisms underlying the paradox of a ouabain-resistant state with elevated endogenous ouabain, suppressed arterial sodium calcium exchange, and low blood pressure. *Am J Physiol Heart Circ Physiol*. 2012;302:H1317–1329.
34. Li J, Khodus GR, Kruusmägi M, et al. Ouabain protects against adverse developmental programming of the kidney. *Nat Commun*. 2010;1:42.
35. Pasdois P, Quinlan CL, Rissa A, et al. Ouabain protects rat hearts against ischemia-reperfusion injury via pathway involving src kinase, mitoKATP, and ROS. *Am J Physiol Heart Circ Physiol*. 2007;292:H1470–1478.
36. Dvela-Levitt M, Ami HC, Rosen H, et al. Ouabain improves functional recovery following traumatic brain injury. *J Neurotrauma*. 2014;31:1942–1947.
37. Peired A, Angelotti ML, Ronconi E, et al. Proteinuria impairs podocytes regeneration by sequestering retinoic acid. *J Am Soc Nephrol*. 2013;24:1756–1768.
38. Mundel P, Reiser J. Proteinuria: an enzymatic disease of the podocyte? *Kidney Int*. 2010;77:571–580.
39. Jefferson JA, Pippin JW, Shankland SJ. Experimental models of membranous nephropathy. *Drug Discov Today Dis Models*. 2010;7:27–33.
40. Cybulsky AV, Quigg RJ, Salant DJ. Experimental membranous nephropathy redux. *Am J Physiol Renal Physiol*. 2005;289:F660–671.
41. Amsellem S, Gburek J, Hamard G, et al. Cubulin is essential for albumin reabsorption in the renal proximal tubule. *J Am Soc Nephrol*. 2010;21:1859–1867.
42. Khan S, Abu Jawdeh BG, Goel M, et al. Lipotoxic disruption of NHE1 interaction with PI(4,5)P2 expedites proximal tubule apoptosis. *J Clin Invest*. 2014;124:1057–1068.
43. Lau GJ, Godin N, Maachi H, et al. Bcl-2-modifying factor induces renal proximal tubular cell apoptosis in diabetic mice. *Diabetes*. 2012;61:474–484.
44. Dizin E, Hasler U, Nlandu-Khodo S, et al. Albuminuria induces a proinflammatory and profibrotic response in cortical collecting ducts via the 24p3 receptor. *Am J Physiol Renal Physiol*. 2013;305:1053–1063.
45. Galluzzi L, Aaronson SA, Abrams J, et al. Guidelines for the use and interpretation of assays for monitoring cell death in higher eukaryotes. *Cell Death Differ*. 2009;16:1093–1107.
46. Su J, Li SH, Chen ZH, et al. Evaluation of podocytes lesion in patients with diabetic nephropathy: Wilms' tumor-1 protein used as a podocyte marker. *Diabetes Res Clin Pract*. 2010;87:167–175.
47. Zhang S, Malmersjo S, Li J, et al. Distinct role of the N-terminal tail of the Na,K-ATPase catalytic subunit as a signal transducer. *J Biol Chem*. 2006;281:21954–21962.
48. Oken DE, Flamenbaum W. Micropuncture studies of proximal tubule albumin concentrations in normal and nephrotic cells. *J Clin Invest*. 1971;50:1498–1505.
49. Larsson SH, Larsson L, Lechene C, Aperia A. Studies of terminal differentiation of electrolyte transport in the renal proximal tubule using short-term primary cultures. *Pediatr Nephrol*. 1989;3:363–368.
50. Benigni A, Gagliardini E, Remuzzi A, et al. Angiotensin-converting enzyme inhibition prevents glomerular-tubule disconnection and atrophy in passive Heymann nephritis, an effect not observed with a calcium antagonist. *Am J Pathol*. 2001;159:1743–1750.
51. Chang AM, Ohse T, Krofft RD, et al. Albumin-induced apoptosis of glomerular parietal epithelial cells is modulated by extracellular signal-regulated kinase 1/2. *Nephrol Dial Transplant*. 2012;27:1330–1343.
52. Okamura K, Dummer P, Kopp J, et al. Endocytosis of albumin by podocytes elicits an inflammatory response and induces apoptotic cell death. *PLoS One*. 2013;8:e54817.
53. Matsusaka T, Kobayashi K, Kon V, et al. Glomerular sclerosis is prevented during urinary tract obstruction due to podocyte protection. *Am J Physiol Renal Physiol*. 2011;300:F792–F800.
54. Wiggins RC. The spectrum of podocytopathies: a unifying view of glomerular diseases. *Kidney Int*. 2007;71:1205–1214.
55. Kale S, Karihaloo A, Clark P, et al. Bone marrow stem cells contribute to repair of the ischemically injured renal tubule. *J Clin Invest*. 2003;112:42–49.
56. Duffield JS, Park KM, Hsiao LL, et al. Restoration of tubular epithelial cells during repair of the postischemic kidney occurs independently of bone marrow-derived stem cells. *J Clin Invest*. 2005;115:1743–1755.
57. MacKenzie SH, Schipper JL, Clark AC. The potential for caspases in drug discovery. *Curr Opin Drug Discov Devel*. 2010;13:568–576.
58. del Nogal M, Luengo A, Olmos G, et al. Balance between apoptosis or survival induced by changes in extracellular matrix composition in human mesangial cells: a key role for ILK-NFκB pathway. *Apoptosis*. 2012;17:1261–1274.
59. Oliver J. The aglomerular nephrons of terminal Bright's disease. In: Oliver J, ed. *Architecture of the Kidney in Chronic Bright's Disease*. New York, NY: Paul B. Hoeber; 1937:43–57.
60. Gibson IW, Downie TT, More IAR, Lindop GB. Atubuli glomeruli and glomerular cysts–a possible pathway for nephron loss in the human kidney? *J Pathol*. 1996;179:421–426.
61. Forbes MS, Thornhill BA, Galarreta CI, et al. Chronic unilateral obstruction in the neonatal mouse delays maturation of both kidneys and leads to late formation of atubular glomeruli. *Am J Physiol Renal Physiol*. 2013;305:F1736–F1764.
62. Galarreta CI, Grantham JJ, Forbes MS, et al. Tubular obstruction leads to progressive proximal tubular injury and atubular injury and atubular glomeruli in polycystic kidney disease. *Am J Pathol*. 2014;184:1957–1966.
63. Bolden JE, Peart MJ, Johnstone RW. Anticancer activities of histone deacetylase inhibitors. *Nat Rev Drug Discov*. 2006;5:769–784.
64. Czaja AJ. Targeting apoptosis in autoimmune hepatitis. *Dig Dis Sci*. 2014;59:2890–2904.
65. Eddy AA. The origin of scar-forming kidney myofibroblasts. *Nat Med*. 2013;19:964–966.
66. Papasotiriou M, Genovese F, Klinkhammer BM, et al. Serum and urine markers of collagen degradation reflect renal fibrosis in experimental kidney diseases. *Nephrol Dial Transplant*. 2015;30:1112–1121.
67. Johnson A, Di Pietro LA. Apoptosis and angiogenesis: an evolving mechanism for fibrosis. *FASEB J*. 2013;27:3893–3901.

68. Wang K, Lin B, Brems JJ, Garnelli RL. Hepatic apoptosis can modulate liver fibrosis through TIMP1 pathway. *Apoptosis*. 2013;18:566–577.
69. Spender LC, Carter MJ, O'Brien DI, et al. Transforming growth factor-β directly induces p53-upregulated modulator of apoptosis (PUMA) during the rapid induction of apoptosis in Myc-driven B-cell lymphomas. *J Biol Chem*. 2013;288:5198–5209.
70. Fan Y, Xiao W, Li Z, et al. RTN1 mediates progression of kidney disease by inducing ER stress. *Nat Commun*. 2015;6:7841.
71. Gentle ME, Shi S, Daehn I, et al. Epithelial cell TGFβ signaling induces acute tubular injury and interstitial inflammation. *J Am Soc Nephrol*. 2013;24:787–799.
72. Celsi G, Jakobsson B, Aperia A. Influence of age on compensatory renal growth in rats. *Pediatr Res*. 1986;20:347–350.
73. Mendonça AC, Oliveira EA, Fróes BP, et al. A predictive model of progressive chronic kidney disease in idiopathic nephrotic syndrome. *Pediatr Nephrol*. 2015;30:2011–2020.
74. Khan F, Spicarová Z, Zelenin S, et al. Negative reciprocity between angiotensin II type 1 and dopamine D1 receptors in rat renal proximal tubule cells. *Am J Physiol Renal Physiol*. 2008;295: F1110–F1116.
75. Lal MA, Andersson AC, Katayama K, et al. Rhophilin-1 is a key regulator of the podocytes cytoskeleton and is essential for glomerular filtration. *J Am Soc Nephrol*. 2015;26:647–662.
76. Große L, Wurm CA, Brüser C, et al. Bax assembles into large ring-like structures remodeling the mitochondrial outer membrane in apoptosis. *EMBO J*. 2016;35:402–413.